Phase transitions in Langmuir monolayers of polar molecules

David Andelman

Corporate Research Science Laboratories, Exxon Research and Engineering Company, Annandale, New Jersey 08801 and Physique de la Matière Condensée, Collège de France, 75231 Paris Cedex 05, France

Françoise Broçhard

Physique de la Matière Condensée, Collège de France, 75231 Paris Cedex 05, France

Jean-François Joanny

Département de Physique des Matèriaux, Université C. Bernard-Lyon I, 69622 Villeurbanne, France

Insoluble Langmuir monolayers are investigated in the presence of dipolar forces which can have two origins: permanent dipoles in neutral monolayers and induced dipoles in charged monolayers. The main effect of the additional long-range repulsive interactions is to stabilize undulating phases at thermodynamic equilibrium. Phase diagrams are obtained in two limits: close to the liquid–gas critical point via a Ginzburg–Landau expansion of the free energy (mainly within a mean-field approximation), and at low temperatures by free energy minimization. Possible applications of this theory to experiments at the liquid–gas, liquid expanded–liquid condensed, and solid–liquid transitions are discussed.

I. INTRODUCTION

Many amphiphile molecules (surfactants, fatty acids, or lipids) form insoluble monolayers at the water/air interface. The phase diagram of these Langmuir monolayers has been extensively studied by surface tension measurements or with Langmuir troughs and often shows a rich variety of phases.[1]

At very low surface pressure (<0.1 mN/m) the surface concentration is small and the monolayer is in a gaseous state. In this state the area occupied by one molecule is much larger than the polar head area and it is generally assumed that the tails of the molecules lie on the water/air interface.

An increase in the surface pressure, in some cases, induces a liquid–gas transition. This transition has been studied in great detail[2] for pentadecanoic acid by measuring the surface pressure and the area per molecule while keeping the temperature constant. A plateau of such isotherms in the pressure–area plane indicates a coexistence between liquid and gas phases i.e., a first-order transition. Due to the decrease in the area per molecule in the liquid state, the tails of the molecules do not lie flat on the water/air interface and hence have a tendency to point towards the air. As for three-dimensional systems, a critical point is reached upon increasing the temperature. The critical behavior around this liquid–gas critical point seems to be mean-field-like,[2] a phenomenon that is not well understood.

The most striking property of the liquid state is in many cases (with long and flexible molecules) the existence of a *kink* in the pressure–area isotherms. This kink divides the liquid state into two "phases": a liquid-expanded phase at lower concentrations and a liquid-condensed phase at higher concentrations. However, it is not clear whether these phases are two distinct equilibrium phases. Consequently the liquid expanded–liquid condensed transition has been the subject of much controversy both experimentally[3] and theoretically.[4]

In particular, Middleton *et al.*[3] find a plateau in the iso-

therms of pentadecanoic acid, hexadecanoic acid, and dihexadecanoyl phosphatidylcholine (DHPC) at the liquid expanded–liquid condensed transition. They thus conclude that the transition is first order. Moreover, they claim that the absence of a plateau in many experimental studies is due to such artifacts as: retention of the spreading solvent, accumulation of impurities at the interface, nonequilibrium determination of the isotherms, hysteresis effects, or working with undersaturated water vapor pressure.

On the other hand, theoretically, a kink in the isotherms can be produced if the monolayer has two order parameters: the area per polar head and another order parameter which undergoes a transition. Following Langmuir[5] and Kirkwood[6] many lattice-gas theories have been developed[4] where the orientation of the molecular tails is considered as the additional order parameter. Any transition between different orientational states couples to the monolayer concentration and may produce a kink in the isotherm. Such a transition has recently been directly observed in pentadecanoic acid monolayers by Rasing *et al.*[7] using nonlinear optics. In this paper we will argue that in some systems another way of having an additional order parameter can be an undulation of the inplane concentration rather than the orientation of the chains.

Increasing even further the surface pressure of monolayers in the liquid state, induces a liquid–solid transition towards a solid phase where the polar heads are closely packed and the surface compressibility is very small.

In recent years, some very refined experimental techniques that allow a more detailed understanding of monolayers have been developed.[8–12] Abraham *et al.*[8] studied the viscoelastic properties of stearyl alcohol and nanodecanoic acid and were able to determine the shear modulus of the solid phase. McConnell and co-workers[9] and Möhwald and co-workers[10] developed an epifluorescence microscopy technique which allows a direct visualization of the liquid con-

centration in lipid monolayers. A small fraction of lipid molecules are covalently linked to a dye molecule. These labeled molecules are incompatible with the crystalline order and are expelled from the solid phase. Thus the fluorescence occurs only in the liquid phase, and one can observe, at high concentration, an organization of liquid-like and solid-like regions. Both groups[9,10] observed periodic domains (with a hexagonal symmetry) of solid phase in a continuous liquid-phase background. The same epifluorescence technique was also used to study the liquid–gas transition, where the fluorescence is quenched in the gas state due to the contact of the dye molecules with the water.[11]

Some of the properties of monolayers can be explained if electrostatic interactions are also considered.[12,13] They have two origins:

(i) Most neutral surfactant molecules carry a permanent dipole moment which has a preferential orientation perpendicular to the interface.

(ii) Charged monolayers create an electrical double layer which in some cases is equivalent to a layer of permanent dipoles. The intensity of the equivalent dipoles can then be tuned by varying the Debye–Hückel screening length of the double layer or equivalently by changing the ionic strength in the water.

Experimentally, these electrostatic effects are measured by the so-called surface potential.[1,14]

The purpose of this paper is to study theoretically the role of these electrostatic interactions on the phase diagram of insoluble monolayers. In the next section, we study in details the interactions between the dipoles of both charged and neutral monolayers. The competition between these long-range repulsive interactions and the short-range attraction due to van der Waals forces is at the origin of new phases of monolayers where the concentration is not isotropic but rather has periodic (in-plane) oscillations. We consider such *supercrystal* phases with a hexagonal or stripe (lamellar) symmetry.[15] These phases could be related to the periodic domains observed by the fluorescence techniques[9–11] and to the oscillations in the surface potential measured in some other experiments[14,16,17] in the liquid expanded–liquid condensed transition region. On the other hand, it is not clear to what extent these experiments are done in true equilibrium for which our theory applies. In Sec II we analyze the effects of electrostatic interactions. The equilibrium phase diagrams are studied in Sec. III for two limits: close to the liquid–gas critical point and at very low temperatures. Our conclusions and the possible relevance to experiments are presented in Sec. IV.

II. ELECTROSTATIC INTERACTIONS IN INSOLUBLE MONOLAYERS

A. Neutral monolayers

We first study the electrostatic interactions in a Langmuir monolayer of neutral molecules. Each molecule carries a dipole moment μ (of the order of a few mD), that is preferentially oriented perpendicular to the water/air interface while its averaged tangential component vanishes. The two-dimensional polarization is given by $\mathbf{P} = \mu\Phi$, where Φ is the in-plane monolayer concentration. When all the dipoles are immersed in the aqueous liquid (of dielectric constant ϵ) the discontinuity of the potential at the surface is

$$\Delta V = \frac{P}{\epsilon^*} = \frac{\mu\Phi}{\epsilon^*}, \tag{1}$$

ϵ^* represents here the local dielectric constant seen by the dipoles. We will, as a first approximation, neglect the variation of the dielectric constant close to the water/air interface, hence ϵ^* is equal to the bulk dielectric constant ϵ. We now assume that all the dipoles are immersed in the water at a very small distance h from the water/air interface, $z = -h$, and that their surface concentration oscillates with a wave vector q: $\Phi(x) = \Phi_0 + \Phi_q e^{iqx}$ as shown in Fig. 1.

The electrical potential V satisfies the Laplace equation

$$\nabla^2 V = 0 \tag{2}$$

with the following boundary conditions:

(i) $\lim_{z\to\infty} V = \lim_{z\to-\infty} V = 0$.

(ii) $\epsilon(z)\partial V/\partial z$ is continuous at $z = 0$.

(iii) The jump in the potential at $z = -h$ is given by Eq. (1).

In the limit where h goes to zero this Laplace equation is easily solved:

$$
\begin{aligned}
V &= \frac{\mu\Phi_q}{\epsilon + \epsilon_0} e^{-|q||z| + iqx}, \quad z > 0, \\
V &= \frac{-\epsilon_0\mu\Phi_q}{\epsilon(\epsilon + \epsilon_0)} e^{|q||z| + iqx}, \quad z < 0.
\end{aligned}
\tag{3}
$$

The electrostatic free energy of the dipoles subject to this potential V is

$$F_{el} = -\frac{1}{2}\int \mathbf{P} \cdot \mathbf{E}\, d^2\mathbf{r} = -\frac{1}{2}|q|\mu^2\Phi_q^2 \frac{\epsilon_0}{\epsilon(\epsilon + \epsilon_0)}. \tag{4}$$

A simple interpretation of this result can be given in terms of image dipoles. A given dipole at a distance $z = -h$ from the interface has an image dipole, $\mu' = \mu(\epsilon_0 - \epsilon)/(\epsilon_0 + \epsilon)$, located at $z = h$. Another "real" dipole located at a distance r from the first one sees the field created by both dipoles, $\mu + \mu'$. The interaction energy between the two real dipoles is then

$$g(r) = \frac{\mu^2\epsilon_0}{2\pi r^3\epsilon(\epsilon + \epsilon_0)} \tag{5}$$

which by Fourier transform gives back the free energy, Eq. (4).
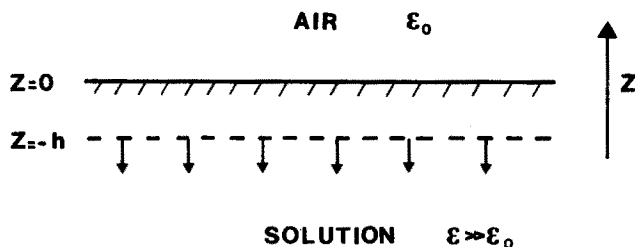
The dipolar interaction energy $g(r)$ is long range and

FIG. 1. A flat interface at $z = 0$ separates air (dielectric constant ϵ_0) from an aqueous solution ($\epsilon \gg \epsilon_0$). Dipoles are confined to the plane $z = -h$.

repulsive (all dipoles point in the same direction along the z axis). Another important feature is the role played by the dielectric constant ϵ ($\gg \epsilon_0$). The energy, Eq. (5), is proportional to ϵ^{-2}. If the dipoles are not immersed in the water, but rather are above the interface at $z = h > 0$, the interaction energy, which is obtained by exchanging ϵ and ϵ_0 in Eq. (5), becomes ϵ independent. Hence, translating the dipoles from just below to just above the interface would increase their interaction by a factor $\epsilon^2 \simeq 6400$. This shows the importance of knowing the value of the actual dielectric constant ϵ^* close to the interface, which is not a very well known parameter.

B. Charged monolayers

We now study a monolayer that is not made of neutral molecules carrying a dipole moment but rather of charged molecules. A first approach is to characterize such a monolayer by the experimentally measured quantity—the surface potential, $\zeta(\Phi)$, as a function of the surface concentration Φ. When the concentration Φ has a fluctuation Φ_q at small wave vector q (smaller than the Debye–Hückel screening length κ^{-1}), the surface potential has a fluctuation $\Delta V = (\partial \zeta / \partial \Phi) \Phi_q$. Equation (1) defines an effective dielectric polarization $P_q = \epsilon \Phi_q \partial \zeta / \partial \Phi$ associated with this fluctuation and the corresponding free energy can be estimated from Eq. (4),

$$F_{el} = -\frac{1}{2}|q|\left(\frac{\partial \zeta}{\partial \Phi}\right)^2 \Phi_q^2 \frac{\epsilon \epsilon_0}{\epsilon + \epsilon_0}. \tag{6}$$

In what follows, we employ a different approach where the electrostatic free energy is calculated directly using the linearized Poisson–Boltzman equation. Each surfactant molecule is assumed to have a charge e and the charges lie on the interface ($z = 0$). The surface charge density is $\sigma = e\Phi$ and the ionic solution is characterized by the Debye–Hückel screening length κ^{-1}. We study a fluctuation of the concentration $\delta\Phi = \Phi_q e^{iqx}$. The electrical potential satisfies the linearized Poisson–Boltzman equation

$$\begin{aligned}\nabla^2 V - \kappa^2 V = 0, &\quad z < 0, \\ \nabla^2 V = 0, &\quad z > 0,\end{aligned} \tag{7}$$

with the boundary conditions

(i) $\lim_{z \to \infty} V = \lim_{z \to -\infty} V = 0$.

(ii) $-\epsilon_0 (\partial V/\partial z)_{z\uparrow 0} + \epsilon (\partial V/\partial z)_{z\uparrow 0} = e\Phi_q e^{iqx}$.

(iii) The potential is continuous at $z = 0$.

For a charge fluctuation at a wave vector q, the effective screening length $1/\kappa'$ is such that

$$\kappa'^2 = \kappa^2 + q^2 \tag{8}$$

and the electric potential is

$$V = \frac{e\Phi_q}{\epsilon\kappa' + \epsilon_0|q|} e^{-|q|z + iqx} \quad \text{in the air, } z > 0,$$

$$V = \frac{e\Phi_q}{\epsilon\kappa' + \epsilon_0|q|} e^{|\kappa'|z + iqx} \quad \text{in the solution, } z < 0.$$

The electrostatic energy of the amphiphile molecules is

$$F_{el} = \frac{1}{2}e\Phi_q V(z = 0) = \frac{e^2\Phi_q^2}{2(\epsilon\kappa' + \epsilon_0|q|)}.$$

Two limits should be distinguished at this point: the limit of small wave vectors, $|q| \ll \kappa$, where the charged monolayer can be described by effective dipole moments and the electrostatic free energy is very similar to Eq. (4). In the other limit of large wave vectors, $|q| \gg \kappa$, the electrostatic interactions are not screened and are Coulomb-like rather than dipole-like.

1. Dipolar regime: Strong ionic solution ($|q| \ll \kappa$)

The electrostatic free energy can be expanded as

$$F_{el} \simeq \frac{e^2\Phi_q^2}{2\epsilon\kappa}\left(1 - \frac{\epsilon_0}{\epsilon}\frac{|q|}{\kappa}\right). \tag{9}$$

The first term is the correction to the average energy of the double layer and the second one is the dipolar term. Comparing Eqs. (9) and (4) we conclude that in this limit, $|q| \ll \kappa$, as proposed above, a charged monolayer is equivalent to a neutral monolayer of molecules carrying an effective dipole

$$\mu = \frac{e}{\kappa}\left|1 + \frac{\epsilon_0}{\epsilon}\right|^{1/2}. \tag{10}$$

It is interesting to compare this result with the result of Eq. (6) where we had forced an equivalent dipole density P_q. Equation (6) combined with the value of the surface potential of the electrical double layer $\zeta(\Phi) = e\Phi/\epsilon\kappa$ predicts an equivalent dipole moment $\mu = e/\kappa$. The small difference ($\epsilon \gg \epsilon_0$) between the results stresses again the need to know in details the effective dielectric constant ϵ close to the water/air interface.

The effective dipole moment of charged monolayers given by Eq. (10) (for $\kappa^{-1} \simeq 10$ Å) is, in general, much larger than the dipole moment of neutral molecules (which are of the order of a few mD), and thus the dipolar interactions can have a much stronger effect on the phase diagram of charged monolayers (as is discussed below). Moreover, the dipole moment can be tuned by changing the Debye–Hückel screening length, i.e., the ionic strength in the aqueous solution.

2. Coulomb regime: Weak ionic solution ($|q| \gg \kappa$)

In this regime the electrostatic free energy is

$$F_{el} \simeq \frac{e^2\Phi_q^2}{2|q|(\epsilon + \epsilon_0)}. \tag{11}$$

Note that $|q|^{-1}$ is, in two dimensions, the Fourier transform of $1/(2\pi r)$. This interaction between molecules is thus purely Coulombic and repulsive; screening is not efficient in this regime. We will not study low ionic strength solutions for which this regime can be important, but one could expect in such cases formation of Wigner crystals similar to the two-dimensional colloidal crystals studied by Pieranski.[18]

III. PHASE TRANSITIONS
A. Ginzburg–Landau expansion close to a critical point

In the previous section, some of the effects of dipolar interactions were discussed. We now take into account these long-range repulsive interactions in order to obtain the various equilibrium phases of the system and the transitions between them. We start[15] by considering the Flory–Hug-

gins[19] theory ordinarily used to describe polymer solutions. For an insoluble monolayer the free energy per unit area is

$$\frac{f_0}{kT} = \frac{1}{N}\Phi \log \Phi + \left(\frac{1}{\Sigma_0} - \Phi\right)\log\left(\frac{1}{\Sigma_0} - \Phi\right)$$
$$+ \chi\Phi(1 - \Phi\Sigma_0). \qquad (12)$$

The first two terms describe the entropy of mixing of surfactant molecules on the water/air interface. The parameter $N(>1)$ is the number of Σ_0 (area per polar head) that each surfactant molecule occupies if it lies flat on the water/air interface. Introducing N as a parameter is clearly an approximation because in the "liquid state" the hydrophobic tails stick out of the water while in the "gas state" they tend to lie on the water surface. Thus, effectively, we do not consider the additional degree of freedom of ordering of the tails. However, the advantage of introducing $N > 1$ is that the resulting coexistence curves are asymmetric as seen in experiments.[2] The third term in Eq. (12) with $\chi > 0$ is the enthalpy of mixing and it consists mainly of short range interactions. The average dipole–dipole repulsion will lower χ without changing its sign.

The free energy, Eq. (12), has a coexistence curve separating dilute gas-like region from a denser liquid-like one via a first-order phase transition. This coexistence curve ends with a critical point: $\Phi_c = 1/\{(1 + \sqrt{N})\Sigma_0\}$, and $\chi_c = (1 + \sqrt{N})^2/2N$. In the proximity of the critical point (Φ_c,χ_c) we can expand f_0 in powers of $\Psi = \Phi - \Phi_c$,

$$\frac{f_0 - f_c}{kT} = \frac{1}{2}\alpha\Psi^2(\mathbf{r}) + \frac{1}{4}u\Psi^4(\mathbf{r}) \qquad (13)$$

with

$$\alpha = 2(\chi_c - \chi)\Sigma_0 \propto T - T_c$$

and

$$u = \frac{1}{3\Sigma_0\Phi_c[(1/\Sigma_0) - \Phi_c]^3}. \qquad (14)$$

[There is no Ψ^3 term in Eq. (13) because we took χ as Φ independent in Eq. (12)].

Adding the dipolar interactions (introduced in the previous sections) to the free energy requires that the spatial variation of the monolayer concentration should be taken explicitly into account. Close to the critical point introduced above, it is convenient to remain in the framework of the Landau expansion and to add to Eq. (13) spatially varying terms. The resulting free energy is known as a Ginzburg–Landau expansion and has in our case two additional terms:

(i) An electrostatic contribution coming from dipole-dipole interactions between the polar heads. From Eqs. (4) and (5) this additional free energy can be written as

$$F_{el} = -\frac{1}{2}\int \mathbf{P} \cdot \mathbf{E}\, d^2\mathbf{r} = \frac{1}{2}\int \Psi(\mathbf{r})g(|\mathbf{r} - \mathbf{r}'|)x$$
$$\times \Psi(\mathbf{r}')d^2\mathbf{r}\, d^2\mathbf{r}' \qquad (15)$$

with

$$g(r) = \frac{kT}{2\pi}\left(\frac{b}{r}\right)^3$$

given by Eq. (5) where

$$b^3 = \frac{1}{kT}\frac{\mu^2\epsilon_0}{\epsilon(\epsilon + \epsilon_0)}. \qquad (16)$$

The dipole μ is either a permanent dipole, Eqs. (4) and (5), or an induced dipole, Eq. (10).

(ii) A second term that opposes inplane undulations of the monolayer concentration and is proportional to $(\nabla\Psi)^2$. It expresses the additional cost in energy as one creates inplane perturbations of an isotropic Ψ,

$$\frac{F_I}{kT} = \frac{1}{2}\Sigma_0^2\int(\nabla\Psi)^2\, d^2\mathbf{r}. \qquad (17)$$

In Fourier space $\Psi(\mathbf{r}) = \Sigma_q\Phi_q \exp(i\mathbf{q} \cdot \mathbf{r})$ and

$$\frac{F_{el} + F_I}{kT} = \frac{1}{2}\sum_q(\Sigma_0^2 q^2 - b^3|q|)\Phi_q^2. \qquad (18)$$

Note that $\Psi(\mathbf{r})$ and $\Phi(\mathbf{r})$ have the same Fourier components, $\{\Phi_q\}$ except for $q = 0$ where $\Psi_0 = \Phi_0 - \Phi_c$. It is clear that due to the competition between F_{el} and F_I, there is an optimum q vector that minimizes their sum, Eq. (18), and whose magnitude is given by

$$|q^*| = \frac{b^3}{2\Sigma_0^2}. \qquad (19)$$

The two most basic solutions[20] with undulations are:
(i) The smectic phase,

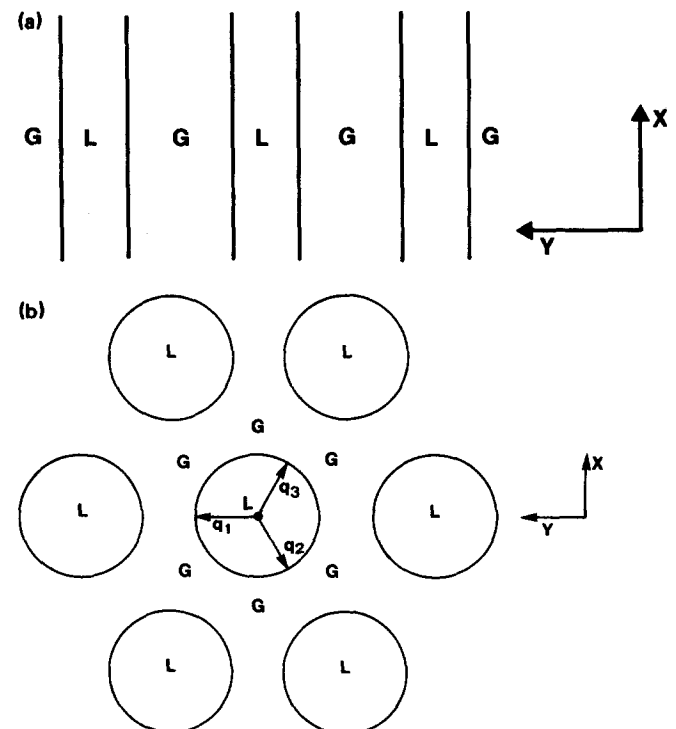$$\Psi_s = \Psi_0 + \Phi_{q^*} \cos q^*y. \qquad (20a)$$

FIG. 2. (a) The stripe phase is shown schematically, where the stripes are chosen to be along the x direction. Domain walls (which are sharp only at low temperatures) separate denser liquid (L) from dilute gas (G). Close to a critical point, the density profile is rather sinusoidal and is given by Eq. (20a). (b) The hexagonal phase is shown schematically. Denser liquid "bubbles" (L) are separated via domain walls from a dilute gas background (G). Domain walls are sharp only at low temperatures. Close to T_c, the density profile is rather given by Eq. (20b) where the three-vector basis is shown for the central bubble.

Here the undulations occur only along one direction in the (x,y) plane as is shown in Fig. 2(a).

(ii) The hexagonal phase,

$$\Psi_H = \Psi_0 + \sum_{i=1}^{3} \Phi_{q^*} \cos(\mathbf{k}_i \cdot \mathbf{r}_i + \delta_i),$$

with

$$|\mathbf{k}_i| = q_0, \quad \sum_{i=1}^{3} \mathbf{k}_i = 0. \tag{20b}$$

Here the undulations are supercomposed in three different directions, as is shown in Fig. 2(b).

These phases were previously considered theoretically by Brazovskii[21] and by Garel and Doniach[22] for thin uniaxial magnetic films. An analogy exists between Langmuir monolayers with polar molecules and thin uniaxial ferromagnetic films subject to a perpendicular magnetic field where stripe (smectic) and hexagonal ("bubble") phases were observed in the past.[23] Studying this magnetic analog of our system, Garel and Doniach[22] obtained a very similar Ginzburg–Landau expansion for the free energy. The only difference between the two free energies is the different origin of the dipolar interactions; in the magnetic film it arises from the demagnetizing contribution due to the finite thickness of the film. In the monolayer the dipoles are permanent and the phenomenon exists even for true two-dimensional film.

Substituting the two proposed solutions. Eqs. (20a) and (20b), into our free energy, Eqs. (13)–(18), we get the two corresponding free energy densities. For the smectic solution

$$\frac{f_S}{kT} = \frac{\alpha}{2}\Psi_0^2 + \frac{u}{4}\Psi_0^4 + \frac{1}{4}\Phi_{q^*}^2$$
$$\times \left(\alpha - \frac{1}{4}\eta^2 + 3u\Psi_0^2 + \frac{3}{8}u\Phi_{q^*}^2 \right), \tag{21}$$

where

$$\eta^2 \equiv \frac{b^6}{\Sigma_0^3} = 4\Sigma_0(q^*)^2$$

is a dimensionless parameter characterizing the dipolar interactions. For the hexagonal solution

$$\frac{f_H}{kT} = \frac{\alpha}{2}\Psi_0^2 + \frac{u}{4}\Psi_0^4 + \Phi_{q^*}^2\left(\frac{3}{4}\alpha - \frac{3}{16}\eta^2 + \frac{9}{4}u\Psi_0^2 \right)$$
$$+ \frac{3}{2}u\Psi_0\Phi_{q^*}^3 + \frac{45}{32}u\Phi_{q^*}^4. \tag{22}$$

Notice that the appearance of the cubic term $(\Phi_{q^*})^3$ in Eq. (22) is a special feature of the hexagonal phase which has a three-vector basis, Eq. (20b), and corresponds to an adequate choice of the phases, $\Sigma\delta_i = 0$.

We define the following reduced dimensionless parameters:

$$\delta \equiv \frac{4\alpha}{\eta^2}, \quad m_0^2 \equiv \frac{4u}{\eta^2}\Psi_0^2, \quad m_{q^*}^2 \equiv \frac{u}{\eta^2}\phi_{q^*}^2. \tag{23}$$

Dividing the various free energy densities by $\eta^4/16u$, results in the following dimensionless free energies:

$$f_S = \frac{\delta}{2}m_0^2 + \frac{1}{4}m_0^4 + m_{q^*}^2(\delta - 1 + 3m_0^2) + \frac{3}{2}m_{q^*}^4, \tag{24a}$$

$$f_H = \frac{\delta}{2}m_0^2 + \frac{1}{4}m_0^4 + m_{q^*}^2(3\delta - 3 + 9m_0^2 + 12m_0m_{q^*})$$
$$+ \frac{45}{2}m_{q^*}^4. \tag{24b}$$

The isotropic solution is obtained by taking $m_{q^*} = 0$ in Eqs. (24), yielding

$$f_I = \frac{\delta}{2}m_0^2 + \frac{1}{4}m_0^4.$$

Phase diagrams can be constructed by looking for the absolute minimum of f_i-μm_0, where the subscript i stands for S (stripe), H (hexagonal), and I (isotropic), and μ being the chemical potential coupled to the average overall concentration, $\langle m \rangle = m_0$.

Minimizing f_S f_H, and Eqs. (24) with respect to m_{q^*} we get that the stripe phase exists only for

$$3m_0^2 < 1 - \delta \tag{25}$$

while the hexagonal phase exists for

$$3m_0^2 < 5(1 - \delta)/4. \tag{26}$$

Minimizing $f_i - \mu m_0$ also with respect to m_0, we obtain numerically the phase diagrams which are shown in Figs. 3 and 4. In Fig. 3 the reduced temperature δ is plotted as a function of the average concentration $m_0 \sim \langle \Phi \rangle - \Phi_c$. All the first-order transition lines terminate at a special critical point $(m_0^* = 0, \delta^* = 1)$. Close enough to δ^*, there are five distinct phases: an isotropic dilute gas (G), a dilute hexagonal phase that consists of droplets of liquid in gas (H), a stripe (S), a dense (inverted) hexagonal phase that consists of droplets of gas in liquid (IH), and a dense liquid phase (L). Between these five phases there are four regions of two-phase coexistence: G–H, H–S, S–IH, IH–L. At a lower temperature, $\delta \simeq -1.6$, the H and IH phases disappear thus leaving only three distinct phases: G, S, and L, with two coexistence regions between gas and stripe phases, G–S, and between stripe and liquid phases, S–L. Yet at even a lower temperature, $\delta \simeq -4.45$, the stripe phase itself disappears and we are left with the regular liquid–gas coexistence curve which in our reduced variables is simply a parabola $m_0^2 = \delta$. All the other
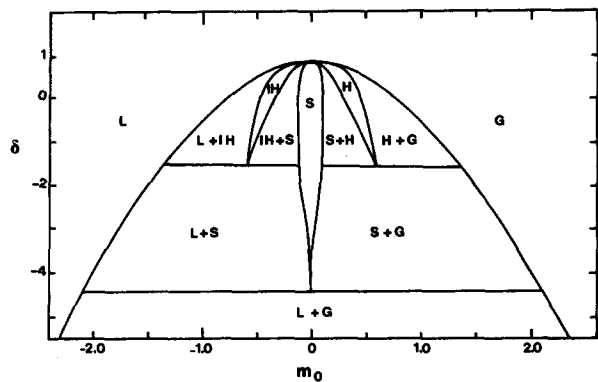

FIG. 3. Phase diagram in the (m_0, δ) plane where $\delta \sim T - T_c$ is the reduced temperature and $m_0 \sim \langle \Phi \rangle - \Phi_c$ is the reduced concentration. The two isotropic phases: liquid (L) and gas (G) are separated by the hexagonal (H), stripe (S), and inverted hexagonal (IH) phases. Two-phase coexistence regions are also indicated. This phase diagram was obtained from Eqs. (24) and is valid only close to $(\delta^* = 1, m_0^* = 0)$.
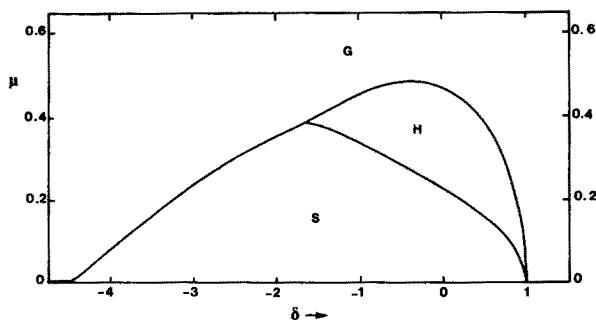
FIG. 4. Phase diagram in the reduced temperature (δ)–chemical potential (μ) plane. This phase diagram is symmetric around $\mu = 0$ thus is shown only for $\mu > 0$. First-order transition lines separate the isotropic dilute gas (G) from hexagonal (H) and stripe (S) phases. This phase diagram was obtained from Eqs. (24) and is valid only close to ($\delta^* = 1$, $m_0^* = 0$).

coexistence curves close to $m_0^* = 0$, $\delta^* = 1$, also scale with an exponent $m_0 \sim \delta^\beta$, $\beta = 1/2$, which is the expected mean-field value for β.

For completeness (and also for comparison with Ref. 22) we plot in Fig. 4 the phase diagram in the reduced temperature–chemical potential plane (δ, μ). At $(\mu = 0, \delta^* = 1)$ there are two first-order transition lines joining up. Thus at lower temperatures these lines separate the five distinct phases that were mentioned before: G, H, S, IH, and L. Around $\delta \cong -1.6$ there is a triple point at $\mu \cong 0.38$ where three first order lines: G–H, H–S, and S–G are joining together. Since our results are symmetric about $\mu = 0$, another triple point exists for $\mu \cong -0.38$. For even lower temperatures the three first-order lines G–S, S–L, and L–G join up at $\mu = 0$, $\delta \cong -4.45$ thus leaving only the regular L–G first-order line at $\mu = 0$ for lower temperatures. We also obtained the phase diagrams where the hexagonal phase was explicitly omitted.[24]

These results that are derived from a Ginzburg–Landau expansion of the dominant q-vector mode are accurate only close to the critical point, $\delta^* = 1$. Far from the critical point other modes have a significant contribution, and the disappearance of stripe and hexagonal phases at lower temperatures could be a fault of this one-mode Ginzburg–Landau expansion. In a low temperature calculation presented below we go to the other extreme limit of a concentration that varies sharply between two given values and show that the stripe phase is more stable than the isotropic phase for some range of concentration.

B. Stability of equilibrium phases at low temperatures

In the previous section we concluded that the disappearance of the undulating phases at lower temperatures, Figs. 3 and 4, is probably related to the approximations that were employed. In this section a low temperature calculation is used in order to show that an undulating phase with sharp domain walls is stable even at zero temperature. Close to a critical point, a Ginzburg–Landau expansion of a single q-vector mode is reasonable since the amplitude of the first harmonic grows faster than that of any higher harmonics.[22] Nevertheless, at low temperatures where domain walls become sharp, all higher harmonics in Eq. (18) have to be

taken into account. Such a calculation at intermediate temperatures is quite complicated and we will rather concentrate in this section on the behavior at low temperature where domains are assumed to have sharp walls (independent of the domain size), Figs. 2, and the entropy terms in the free energy, Eqs. (15)–(17), are partially neglected.

For simplicity a stripe phase with periodicity $D = (D_L + D_G)$ is considered. (The treatment of the hexagonal phases will be left for future investigation.) The concentration of the gas phase (liquid phase) is Φ_G (Φ_L), and the average overall concentration is $\Phi = (D_G \Phi_G + D_L \Phi_L)/(D_G + D_L)$. The dipolar contribution to the total internal energy is given by Eq. (15). For the stripe geometry, the free energy density is

$$\frac{f_{el}}{kT} = \frac{b^3}{\pi a}[x\Phi_L^2 + (1-x)\Phi_G^2] - \frac{b^3}{\pi D}(\Phi_L - \Phi_G)^2$$
$$\times \left[\log \frac{D}{a} + \log x(1-x)\right] + \frac{h(x)}{D}, \quad (27)$$

x is the fraction of the molecules in the liquid state, $x = (\Phi - \Phi_G)/(\Phi_L - \Phi_G) = D_L/D$, and a is a microscopic cutoff provided by the width of the interface between liquid and gas domains. At very low temperatures, $a \cong \sqrt{\Sigma_0}$. Another quantity introduced in Eq. (27) is $h(x)$ which represents the interaction between distant stripes

$$h(x) = \frac{\Phi_L^2 b^3}{\pi}\left[\sum_{p=1}^{\infty} \log \frac{p^2}{p^2 - x^2} + \log(1-x)\right]$$
$$+ \frac{\Phi_G^2 b^3}{\pi}\left[\sum_{p=1}^{\infty} \log \frac{p^2}{p^2 - (1-x)^2} + \log x\right]$$
$$+ \frac{2b^3 \Phi_G \Phi_L}{\pi}$$
$$\times \left[\sum_{p=1}^{\infty} \log \frac{(2p+1)^2 + 4x(1-x) - 1}{(2p+1)^2 - 1}\right]. \quad (28)$$

These interactions between distant stripes are nonsingular [$h(x)$ is a slowly varying function of x, $0 < x < 1$] and have only a small contribution to the overall energy at low temperatures; they renormalize the line tension between gas and liquid phases.

The first two terms in the electrostatic energy, Eq. (27), represent the electrostatic contribution to the osmotic pressure (independent of D) and to the chemical potential of amphiphile molecules. The third and fourth terms in Eq. (27) represents the difference in electrostatic free energy between the stripe phase and two isotropic phases in equilibrium (with the same value of the overall concentration Φ).

A further contribution to the free energy difference Δf between the stripe phase and the isotropic phase comes from the interfacial terms which take into account the concentration variation at each liquid/gas interface. We describe it in terms of a line tension γ which could in principle be calculated from Eqs. (18) and (12) but which will be kept here as a parameter.

The total free energy difference between the stripe and isotropic phases is thus

$$\Delta f = -kT \frac{b^3}{\pi D} (\Phi_L - \Phi_G)^2 \left[\log \frac{D}{a} + \log x(1-x) \right]$$

$$+ \frac{2\gamma + kTh(x)}{D}. \tag{29}$$

The equilibrium period of the stripe structure that minimizes this energy Δf is

$$D = \frac{a}{x(1-x)} \exp(\beta), \tag{30}$$

where β is

$$\beta = \frac{2\pi\gamma^*}{kTb^3(\Phi_L - \Phi_G)^2} + 1$$

$$= \frac{\epsilon^2}{\mu^2\epsilon_0} \frac{2\pi\gamma^*}{(\Phi_L - \Phi_G)^2} + 1 \tag{31}$$

and γ^* is the effective line tension, $\gamma^* = \gamma + kTh(x)/2$. The period D becomes exponentially large whenever $\beta \gg 1$ which seems to be the case far from the critical point and for typical values for the various parameters. However, D depends quite strongly on the precise values of the parameters in Eq. (31). At equilibrium, the free energy density Δf is

$$\Delta f = -kT \frac{b^3}{\pi a} (\Phi - \Phi_G)(\Phi_L - \Phi) \exp(-\beta). \tag{32}$$

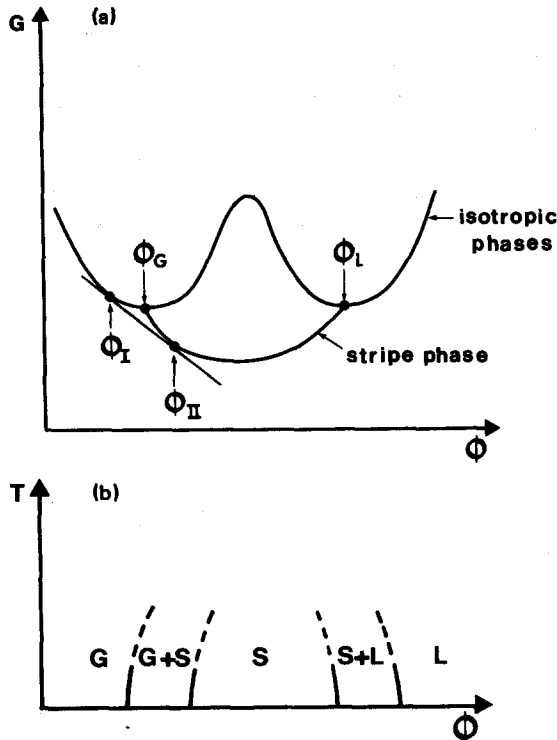We also note that this stabilization of an undulating pat-

G (a)

Φ_G   Φ_L
— isotropic phases

Φ_I

Φ_II   stripe phase

Φ

T (b)

G   'G+S'   S   'S+L'   L

Φ

FIG. 5. (a) The free energy G at low temperatures as a funciton of the concentration Φ is shown schematically. The two isotropic solutions, Φ_G and Φ_L, are the minima of the isotropic free energy. When the dipolar interactions are added, a double tangent construction gives coexistence between Φ_I (isotropic) and Φ_{II} (stripe), both close to Φ_G. Similar two phase coexistence exists close to the liquid phase. (b) The phase diagram for low temperatures is shown schematically in the temperature (T)–concentration (Φ) plane. The stripe phase (S) is stable in the region between the gas (G) and the liquid (L) phases. Two-phase coexistence regions are constructed from (a). They exist between S and L and between S and G. The hexagonal phases are not shown for simplicity.

tern (the fact that $D > 0$ is the optimal solution) is similar to the stripes in solid magnetic films that were mentioned in the previous section and also to the normal field instability that is observed in ferrofluids.[25] There when two immiscible fluids of whom one is ferromagnetic, are placed in a Hele–Shaw geometry and are subject to a normal magnetic field, the system develops a inplane labyrinth pattern on the scale of millimeters. Since the two fluids are completely immiscible, this is similar to our system at very low temperatures.

In order to study the equilibrium between the stripe and the isotropic phases, we consider the thermodynamic potential

$$G = f - \mu_{eq}\Phi + \Pi_{eq},$$

μ_{eq} and Π_{eq} are the chemical potential and osmotic pressure of the two isotropic phases in equilibrium (with concentrations Φ_L and Φ_G). For isotropic phases, $G(\Phi)$ has, by construction, two minima with $G = 0$ for the equilibrium phases: $\Phi = \Phi_L$ and $\Phi = \Phi_G$. Whereas for the stripe phase, $G = \Delta f$. A qualitative plot of G is shown in Fig. 5(a) for these two phases.

The usual double tangent construction, Fig. 5(a), yields the phase diagram shown in Fig. 5(b). An explicit calculation of the equilibrium lines can be made if we neglect the dependence of the interfacial tension γ^* on concentration and if we approximate the variation of G around Φ_L and Φ_G by two parabolas

$$G_G = \tfrac{1}{2}\chi_G^{-1}(\Phi - \Phi_G)^2,$$

$$G_L = \tfrac{1}{2}\chi_L^{-1}(\Phi - \Phi_L)^2,$$

χ_G and χ_L are the osmotic compressibilities of the gas and liquid phases, which should be a good approximation at low temperatures where the energy in the isotropic phases has two deep minima.

On the gas side, for example, when the condition, $\beta \gg 1$ is fulfilled, we find the two equilibrium concentrations

$$\Phi_I \simeq \Phi_G - (\Phi_L - \Phi_G) \frac{kTb^3\chi_G}{\pi a} \exp(-\beta),$$

$$\Phi_{II} \simeq \Phi_G + \frac{\Phi_L - \Phi_G}{2} \left| \frac{2kTb^3\chi_G}{\pi a} \right|^{1/2} \exp(-\tfrac{1}{2}\beta).$$
$$\tag{33}$$

This thus predicts a large single lamellar phase for concentrations between Φ_L and Φ_G and small regions of coexistence between lamellar and isotropic phases around Φ_L and Φ_G.

We have not performed the explicit calculation for the hexagonal phase but it seems reasonable to assume that this phase also remains stable at low temperatures and that over the whole temperature range, the sequence of phases and phase coexistences remains similar to what it is close to the critical point, hence no disappearing of the undulating phases at low temperatures [see Fig. 5(b)].

IV. CONCLUSIONS

We explored the effects of dipolar interactions in Langmuir monolayers. Their main effect is to stabilize supercrystal phases for which the inplane concentration is undulating.

We study here stripe phases (smectic) and to some less extent hexagonal phases (bubbles).

Experimentally, epifluorescence observations have shown the existence of undulating phases in a concentration range which corresponds to the liquid–solid transition. However, for such transitions, the undulating phase is probably due to the nucleation of two dimensional solid regions in a liquid background. Different solid nuclei have different crystalline orientations and are thus separated by grain boundaries which do not disappear even for quite high pressures. The observed hexagonal phases are thus a nonequilibrium phenomenon which cannot be explained only by the equilibrium model presented here. However, since the sizes of the solid domains depend strongly on the ionic strength of the solution, we believe that the electrostatic interactions play a major role in determining the structure of these undulating phases.[12]

The Flory-type theory proposed here is more applicable to fluid phases rather than to the solid–liquid region. This can be both in the liquid–gas or the liquid expanded–liquid condensed regions although due to low surface pressure and concentrations, in the former case fewer effects can be measured. The period of the undulations can be estimated from Eqs. (19), (30) and (31); it can vary from 1000 Å to 1 μm according to the precise magnitude of the dipoles on the surface (or equivalently of the ζ potential). It also depends strongly on the local dielectric constant at the interface which is not very well known.

For charged monolayers, the equivalent dipole can be tuned by varying the ionic strength in the solution. Our theory gives the explicit dependence of the undulation period and the critical temperature as function of the screening length κ^{-1}. However, this does not represent the whole dependence on the ionic strength, since the charge per molecule e also depends strongly on the ionic strength. This must be taken into account when a comparison with experiments is done.

At the liquid expanded–liquid condensed transition, the model does not give a definite explanation for the kink observed in many experiments. It does however demonstrate the role played by an additional order parameter, in our case, the undulations amplitude. As was explained in the introduction, it is not clear if the experimental isotherms show a kink or a more complicated structure as proposed here. Moreover, the jump in the pressure between the two extreme transitions in Fig. 3 is of order of $\epsilon \Delta V^2 / D$, ΔV being the potential jump across the monolayer and D is the period of the undulations. Estimating its magnitude we get a very small value of the order of 0.01 mN/m.

We also make the connection between the dipolar monolayer and two other magnetic systems: a thin uniaxial magnetic film and a thin layer of ferrofluid both subject to a normal magnetic field. In these magnetic analogs, a competition between dipolar forces and domain wall energies or line tension also destabilizes the isotropic state of the system. The ferrofluid is more like our system at $T = 0$ since thermal fluctuations do not play an important role, whereas for the thin magnetic film thermal fluctuations are important. It is striking that the similarity between these three systems exist

although the length scale of the undulations are very different; it can reach a few millimeters in the ferrofluid (subject to magnetic fields of only several hundred Gauss), whereas it can be as small as few hundred Å for the monolayer and in the intermediate micron range for the thin solid magnetic films.

An additional limitation of the theory presented here is that it is a mean field theory and thus it does not take into account correctly critical fluctuations which can be quite important for two-dimensional systems. The effects of these fluctuations have been discussed in details by Brazovskii[21] and by Garel and Doniach.[22] Fluctuations modify the precise shape of the phase diagram especially close to a critical point but the qualitative picture presented here would still remain correct; the transitions are expected to remain first order.[22]

In conclusion it should be noted that the effect of the long-range dipolar forces are important for most of the monolayer properties and not only for the equilibrium phase diagram as was studied in this paper. From an experimental point of view, nonequilibrium phenomena seem to be of particular importance in Langmuir monolayers. Thus the inclusion of dipolar forces in the kinetics of domain growth is of relevance and will be addressed in a separate study.

ACKNOWLEDGMENTS

[1] For a general review see: A. W. Adamson, *Physical Chemistry of Surfaces* (Wiley, New York, 1982); G. L. Gaines, *Insoluble Monolayers at Liquid Gas Interfaces* (Wiley, New York, 1966).

[2] G. A. Hawkins and G. B. Benedek, Phys. Rev. Lett. **32**, 524 (1974); M. W. Kim and D. S. Cannell, *ibid.* **33**, 889 (1975); M. W. Kim and D. S. Cannell, Phys. Rev. A **13**, 411 (1976).

[3] S. R. Middleton, M. Iwasaki, N. R. Pallas, and B. A. Pethica, Proc. R. Soc. London Ser. A **396**, 143 (1984); N. R. Pallas, and B. A. Pethica, Langmuir **1**, 509 (1985).

[4] See, e.g., G. M. Bell, L. L. Combs, and L. J. Dunne, Chem. Rev. **81**, 15 (1981); J. P. Legre, G. Albinet, J. L. Firpo, and A. M. S. Tremblay, Phys. Rev. A **30**, 2720 (1984), and references therein.

[5] I. Langmuir, J. Chem. Phys. **1**, 756 (1933).

[6] J. G. Kirkwood, Publ. Am. Assoc. Advmt. Sci. **21**, 157 (1943).

[7] Th. Rasing, Y. N. Sen, M. W. Kim, and S. Grubb, Phys. Rev. Lett. **55**, 2903 (1985).

[8] B. M. Abraham, K. Miyano, S. Q. Xu, and J. B. Ketterson, Phys. Rev. Lett. **49**, 1643 (1985).

[9] H. M. McConnell, L. K. Tamm, and R. M. Weis, Proc. Natl. Acad. Sci. **81**, 3249 (1984).

[10] M. Lösche and M. Möhwald, Eur. Biophys. **11**, 35 (1985); M. Lösche, E. Sackmann, and M. Möhwald, Ber. Bunsenges. Phys. Chem. **87**, 848 (1983); M. Lösche and M. Möhwald, J. Phys. Lett. (Paris) **45**, L785 (1984).

[11] B. Moore, C. M. Knobler, D. Broseta, and F. Rondelez, J. Chem. Soc., Faraday Trans. 2, **82**, 1753 (1986).

[12] C. A. Helm, L. Laxhuber, M. Lösche, and M. Möhwald, J. Colloid Polym.

Sci. (in press).

[13]P. A. Forsyth, Jr., S. Marcelja, D. J. Mitchell, and B. W. Ninham, Biochem. Biophys. Acta **469**, 335 (1977), and references therein.

[14]M. Plaisance, Ph.D thesis, University of Paris, 1975 (unpublished); M. Plaisance and L. Terminassian-Saraga, C. R. Acad. Sci. (Paris) **270**, 1269 (1970).

[15]D. Andelman, F. Brochard, P. G. deGennes, and J. F. Joanny, C. R. Acad. Sci. (Paris) **301**, 675 (1985).

[16]S. R. Middleton and B. A. Pethica, J. Chem. Soc. Faraday Symp. **16**, 109 (1981).

[17]M. W. Kim and D. S. Cannell, Phys. Rev. A **14**, 1299 (1976).

[18]P. Pieranski, Phy. Rev. Lett. **45**, 569 (1980).

[19]P. Flory, *Principles of Polymer Chemistry*, (Cornell University, Ithaca, 1971).

[20]A cubic phase with fourfold symmetry has always a higher energy in our two-dimensional problem than the smectic one. However, a cubic phase exists for a similar problem of microphase separation of block copolymers in three dimensions: L. Leibler, Macromolecules **13**, 1602 (1980).

[21]S. A. Brazovskii, Zh. Eksp. Teor. Fiz. **68**, 175 (1975) [Sov. Phys. JETP **41**, 85 (1975)].

[22]T. Garel and S. Doniach, Phys. Rev. B **26**, 325 (1982).

[23]The equivalent magnetic problem for thin magnetic films has been considered by C. Kooy and U. Enz, Phillips Res. Rep. **15**, 7 (1960).

[24]If the hexagonal solution is omitted, the resulting phase diagram have both first- and second-order transitions between stripe (S) and the isotropic phases (L and G). These lines meet at a tricritical point, $\delta \cong 0.7$. The mean field theory for a very similar model, the spin one model, was calculated by Blume, Emery, and Griffiths, Phys. Rev. A **4**, 1071 (1971).

[25]R. E. Rosensweig, M. Zahn, and R. Shumovich, J. Mag. Mag. Mat. **39**, 127 (1983); For a review on ferrofluids see R. E. Rosensweig, *Ferrohydrodynamics* (Cambridge University, New York, 1985).